5.2 Dark Layers - A Possible Local Source?

The conventional assumption about the relationship between dark material and depressions is that the material is blown into as well as out of the craters [*Christensen*, 1983; *Jaumann et al.*, 2006] (Fig. 30). Depressions may act as sediment traps into which the aeolian material is blown to accumulate on the depression floor. Once the material is deposited on a crater floor, it may also act as a source, meaning that material is blown out or deflated, frequently in the form of wind streaks [*Thomas et al.*, 1981].

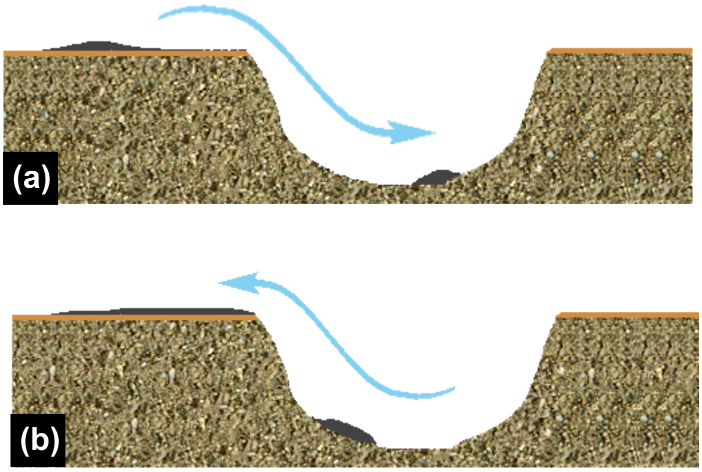

Figure 30: Schematic model of dark material transport into and out of craters.
(a) Dark material is blown into a crater (crater acts as sediment trap). **(b)** Dark material is blown out of a crater (crater acts as sediment source).

In view of the aeolian character of transport and the huge number of traps, it might appear logical at first sight that the trapping function of craters should be the main mechanism that governs the accumulation of dark material. However, HRSC images show that the material is only blown out in most cases (e.g. craters in centre of Fig. 31 middle left). There are just a few examples where aeolian delivery of material from outside a crater can be observed. This is mostly the case in places where a number of craters with dark material lie close to each other and a dark deflational wind streak from an upwind crater reaches its downwind neighbour, delivering material into its interior (e.g. crater in lower left portion of Fig. 31 middle right).
The scarcity of evidence for material being supplied from outside a crater suggests that there must be an alternative material source. Central and western Arabia Terra present good examples for regions, which look completely 'clean' of dark material upwind of the craters. The material solely appears inside and downwind of these craters, forming visible dark dunes and wind streaks. The HRSC orbits 3797_0000 and 1333_0000 shown in Fig. 31 are examples of that situation in Arabia Terra (also described by *Edgett* (2002)). There, it seems that the material has its origin in the crater itself. Fig. 31b and 31c show that the floors of the bigger craters are blotched by numerous smaller craters. It is noticeable that the dark material in these craters solely appears downwind of the smaller craters. The material seems to originate from a sediment source just beneath the crater floor, which was cut open by the smaller craters.

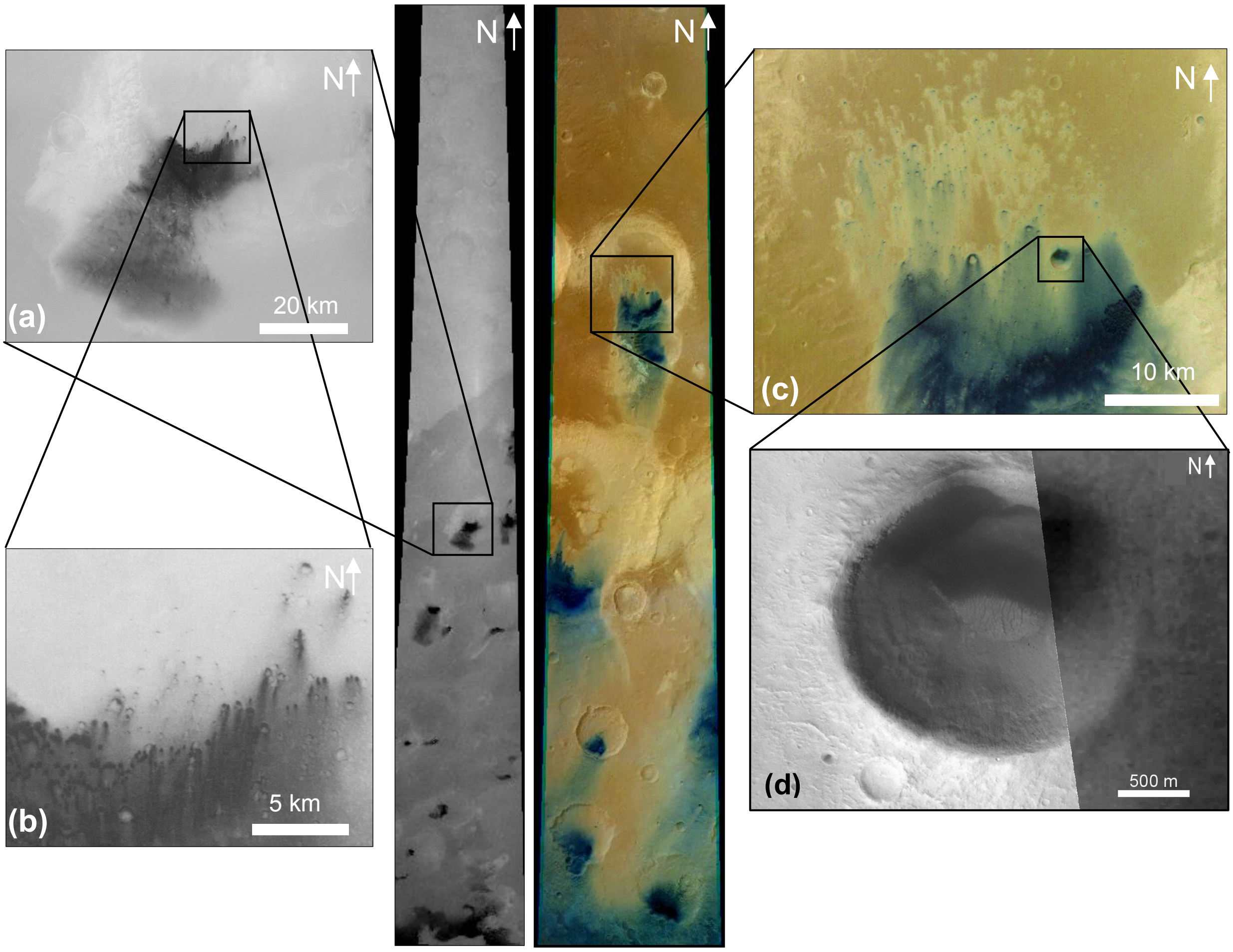

Figure 31: Indication of craters acting as a local material source.
HRSC orbits 1333_0000 **(middle left)** and 3297_0000 **(middle right)** show dark material deposits appearing in the craters and emanating from there. **(a)** Zoom into HRSC 1333_0000 showing the dark patch of a 52 km diameter crater in Arabia Terra (8.9°N, 11.1°E). **(b)** Zoom into the crater floor showing dark material emanating from smaller craters superimposed on the larger crater floor. **(c)** Zoom into HRSC 3297_0000 showing a 62 km diameter crater near Mawrth Vallis (18.9°N, 345.5°E) and dark material emanating from smaller craters. **(d)** Subset of MOC R0701192 overlaid on HRSC showing a small crater comprising a dark layer exposed in the crater wall.

MOC narrow-angle images of small craters (Fig. 31d) reveal dark layers exposed in the crater walls. Such layers can be observed in many other craters. At Rabe Crater (Fig. 32), an intra-crater pit provides illuminating insights into the morphology of the dark layers, as previously described by *Fenton* (2005b). High-resolution images disclose dark gully-like streaks extending down-wall, indicating erosion of these dark layers and a transport of material into the crater's interior (Fig. 32c and 32d) [*Fenton*, 2005b; *Tirsch et al.*, 2007]. HRSC and HiRISE false-colour composites reveal that the blue colour of the dark layers and the gully material resembles that of the dark dune material inside the crater (see Fig. 32 and 33). This colour correlation could suggest that the layers have a mineralogical composition similar to that of the dune material inside the crater. Analyses of corresponding stratigraphic units using colour composites were previously done by *Loizeau et al.* (2007b) and *Loizeau et al.* (2008), proving that this method produces reliable results.

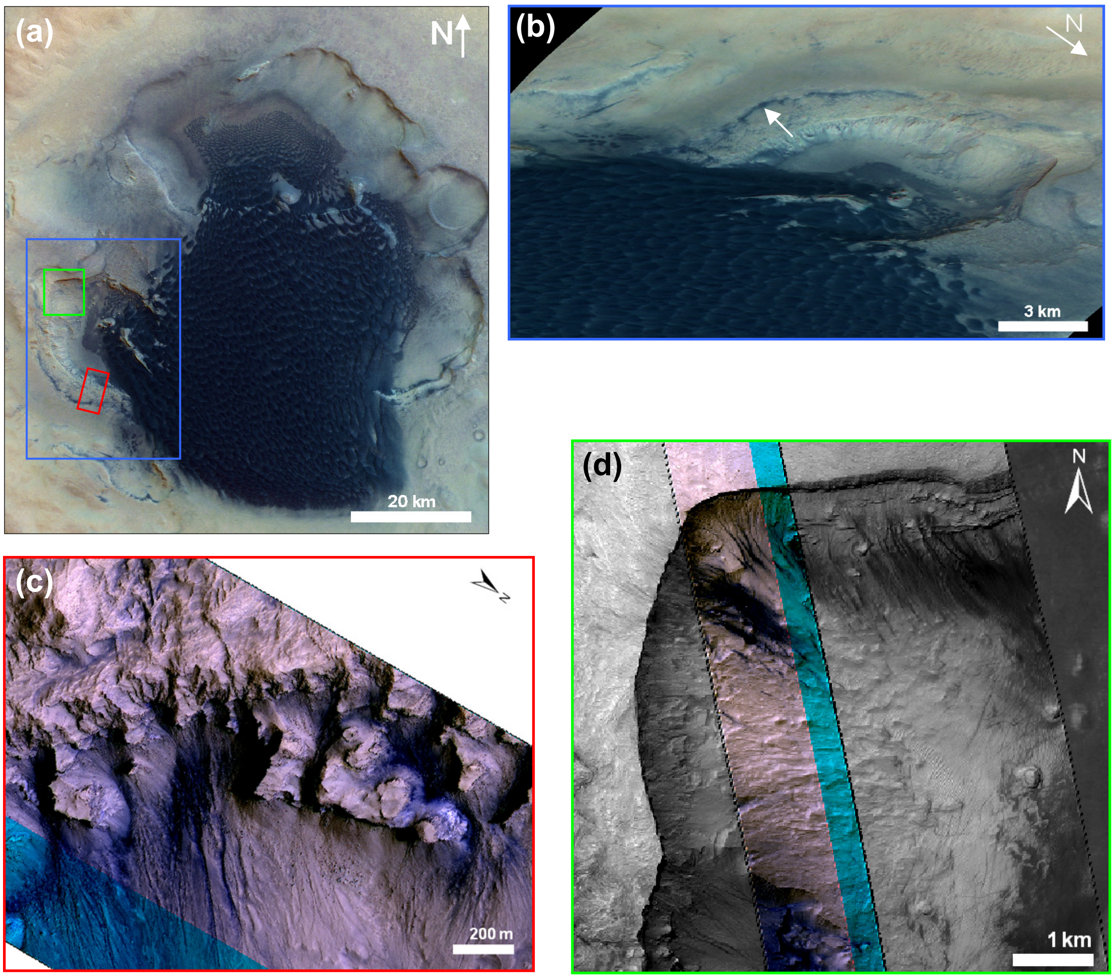

Figure 32: Dark layers exposed in the walls of a pit within Rabe crater.
(a) Plan view of Rabe Crater (43.9°S, 34.8°E; HRSC colour composite 2441_0000), rectangles indicate the positions of Fig. b, c, and d, identifiable by their outline colours. **(b)** Perspective view of the intra-crater pit, same HRSC orbit as Fig. a. **(c)** + **(d)** Dark material emanating from dark layers exposed in the pit wall (subsets of HiRISE colour image PSP 005646_13460, in d: overlaid on red channel of the same image).

The resolution of OMEGA data is not sufficient in most cases to yield reliable information on the spectral characteristics of such small features. However, for Rabe Crater, an olivine composition of the dark layer could be established by OMEGA spectral analysis (see Sect. 5.3.2). Additional high-resolution CRISM data were obtained of some of these dark layers. The spectral analysis of a dark layer at Terra Sirenum is described in Sect. 5.3. It reveals a mafic composition for the dark material emanating from dark layers, which is similar to the mineralogical composition of the dune material. According to this substantive evidence, the dark layers form, where they exist, probably a local source of the dune material inside the craters.

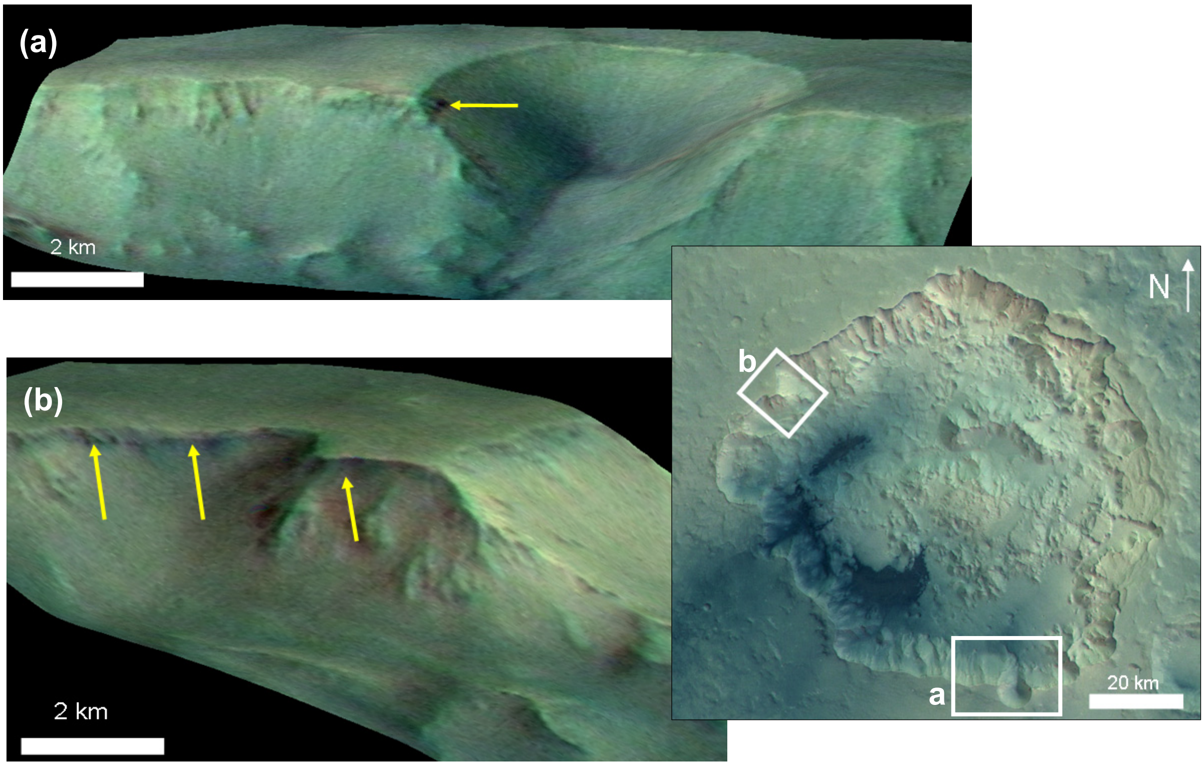

Figure 33: Dark layer exposed in the wall of a possible collapse formation in Ophir Planum (3°S, 307.8°E). The layers exhibit the same false-colour (infrared, green, blue) as the dune material inside the crater (HRSC 0394_0002; rectangles indicate positions of Fig. a & b). Note the aerial correlation between dark layers and the occurrence of dark material within the crater. Compare with the profile in Fig. 29.

An analysis of the image data suggests that there are two ways in which dark layers can be cut by impact craters (Fig. 34). In the first case (A), the layer is cut through by larger impact craters reaching deeper than the level of the dark layer, so that it is exposed in the crater rim (cf. Fig. 32 and 33). In the second case (B), the large impact does not reach the dark layer. However, subsequent smaller impacts that hit the crater floor, reach greater depths, and cut the dark layer in many confined places (cf. Fig. 31). In both cases, mechanical erosion of the dark layers seems to result in a supply of fine-grained intra-crater material. Gravitational transport down-wall and aeolian transport out of the smaller and bigger craters provide the local material distribution.

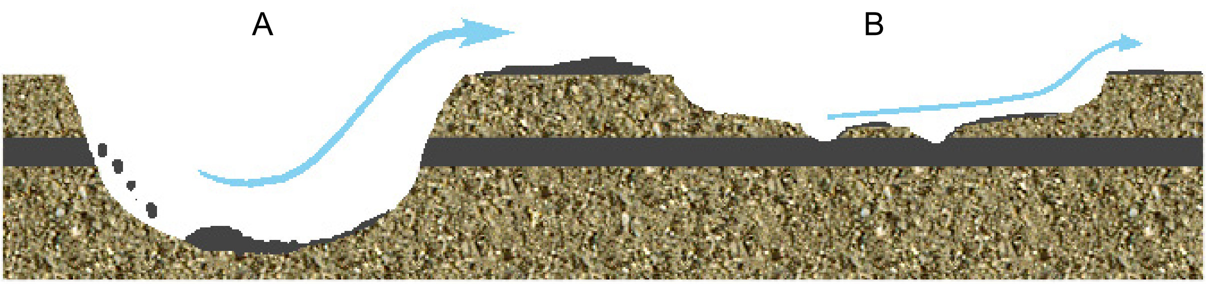

Figure 34: Sketch of two possible cases of exposure of dark material layers indicated by multiple image data. (see text for discussion)

A comparison of the numerous image data indicating exposed dark layers reveals that these dark layers are predominantly situated in the sun-facing walls. In Fig. 31c and 31d as well as in Fig. 35 the dark layers are exposed in the northern wall. Since these images represent northern hemisphere localities, the northern, equator-facing wall is the one that experiences the maximum insolation.

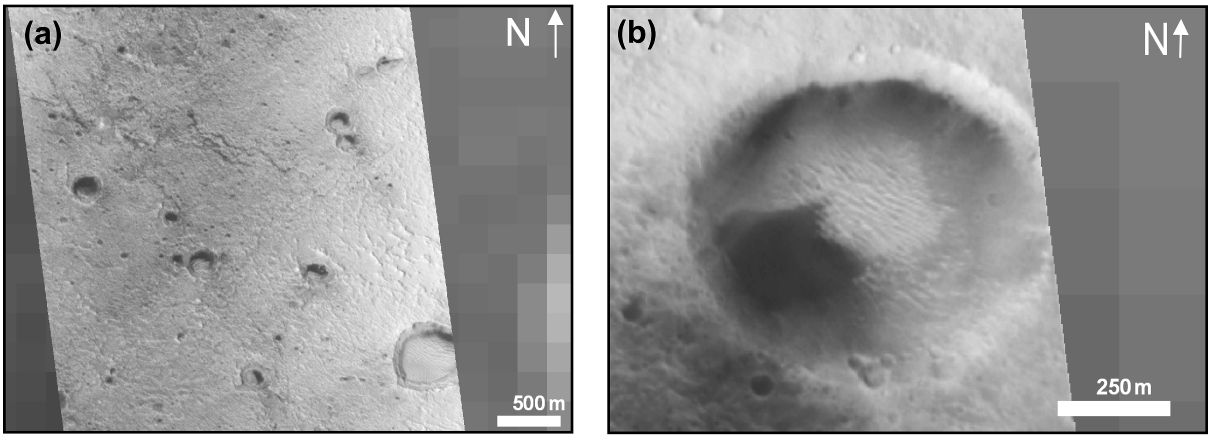

Figure 35: Dark layers exposed in the sun-facing walls of small impact craters in Arabia Terra (near 16.1°N, 344.5°E). **(a)** + **(b)** Subframes of MOC image E0500437.

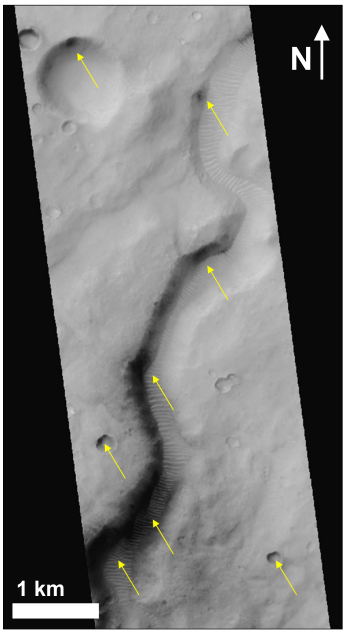

Similar characteristics can be observed in the walls of numerous narrow channel-like structures that are sometimes located in the immediate vicinity of craters and show dark features in their walls, which resemble the layers described above (Fig. 36). This proximity might indicate a generic association between these dark exposures. Further examples were found close to Nili Fossae and in Utopia Planitia, here again, the dark features are exposed in the northern or north-eastern sun-illuminated walls, as shown in Fig. 37a.

Figure 36: Dark features exposed in the walls of channels and craters close to Ares Valles showing remarkable similarity to the dark layers described above (6.8°N, 336.9°E; subset of MOC 2000929).

Roberts et al. (2007) analyzed comparable dark features in the Elysium region and emphasised their exposure in the sun-illuminated walls (Fig. 37b). First noted by *Plescia et al.* (2003), such elongated dark spots are interpreted as deep sunken pits and young eruptive deposits along fissure vents leading to the summit of a volcano. These features are analogues to the Hawaiian fissure vents, which are produced by small-scale fire fountains during volcanic eruptions [*Roberts et al.*, 2007]. The dark halos associated with the dark features are supposed to be pyroclastic/eruptive/fumarole material.

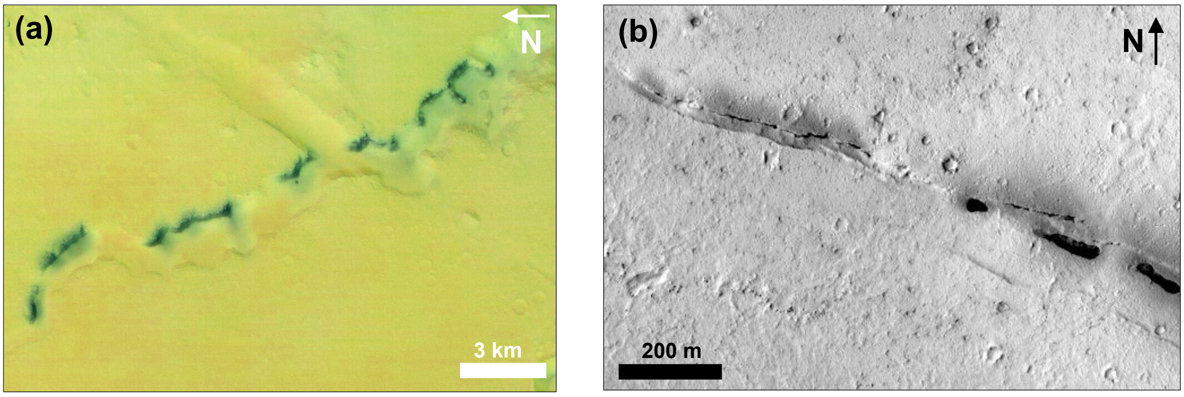

Figure 37: Dark features exposed in the sun-facing walls of channel-like structures.
(a) Probable dark material layer exposed in a channel wall near Nili Fossae (24.3°N, 78.7°E; subset of HRSC 3340_0000). **(b)** Elongated dark spots along a fissure vent in Elysium Planitia (7.9°N, 163.3°E; subset of MOC E0501457 (see text and *Plescia* (2003) and *Roberts et al.* (2007) for discussion).

It is not clear whether the observed dark channel features all have the same generic origin than the layers in the craters. However, the similarity of exposition in the sun-facing wall is remarkable, leading to the assumption that there may be a certain connection between exposure to the sun and the occurrence of these features. In all examples, the opposite pole-facing walls do not show any evidence of dark material emersion. This situation suggests that the exposure of the dark layers in crater walls might be associated with the removal of covering dust supported by warming due to insolation (Fig. 38). The higher temperatures at the sun-illuminated wall might result in the sublimation or melting of the probably ice-cemented superficial crust, which generally covers the dark layers along the crater walls. This could also explain why dark layers are not observable in all crater walls (Fig. 39).

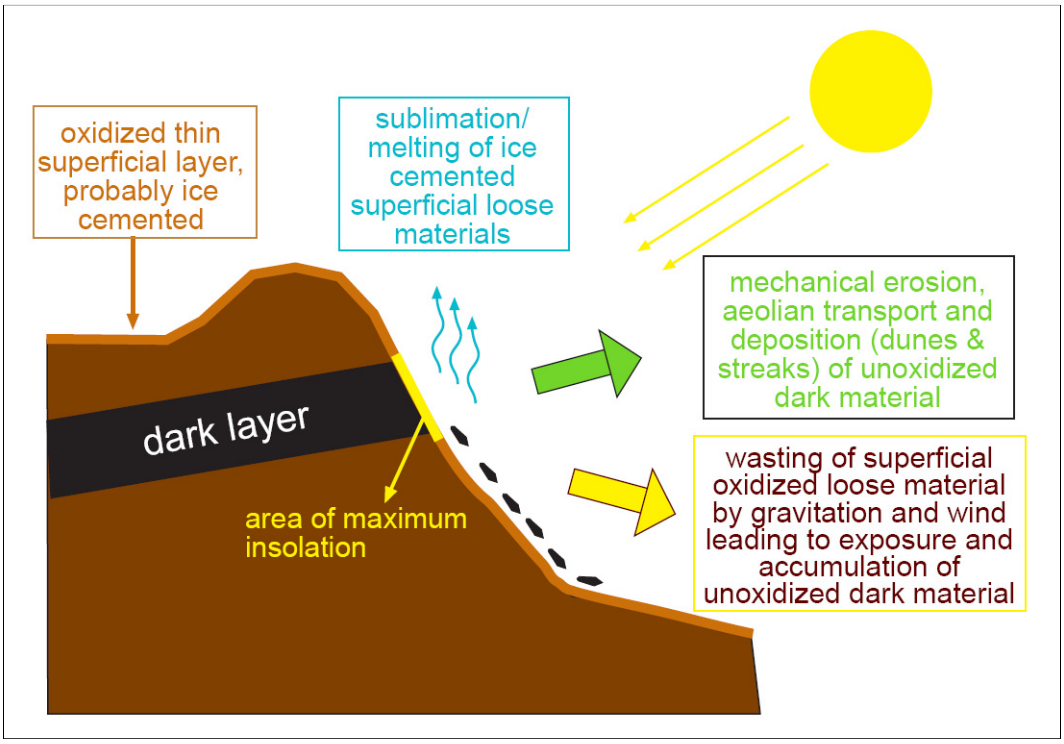

Figure 38: Function diagram of probable processes leading to the exposure of dark layers in crater walls.

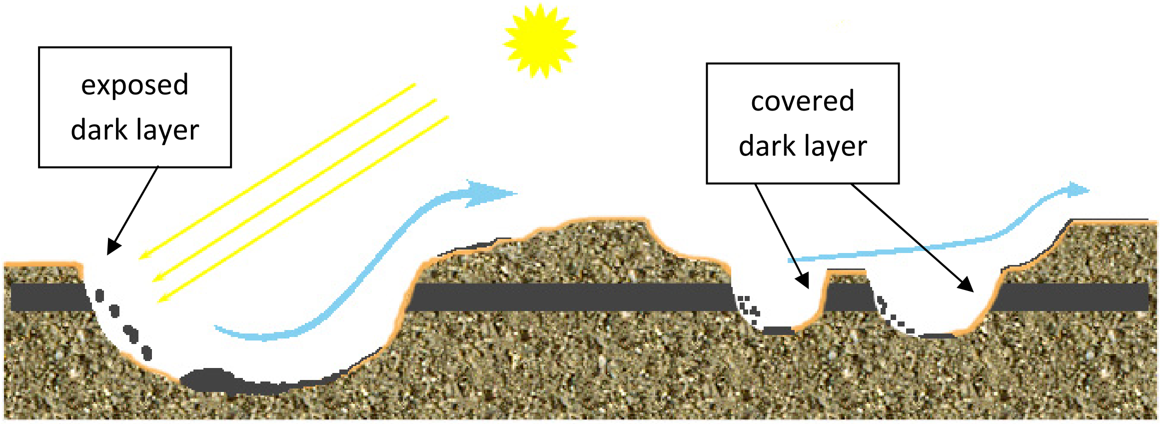

Figure 39: Sketch of probable situations of coverage and exposure of dark layers in crater walls.
In the sun-averted wall, any dark layers are covered by regolith or dust (right). Increased solar irradiation of the opposite wall triggers melting and/or erosion and removal in the superficial material mantling the surface (left).

At the end of this section, the relative elevation of craters with and without dark material exposure will be analyzed, using orbit 3297_0000 to obtain an impression of the elevation conditions. For this analysis, a profile was generated from HRSC DTM data across the entire orbit, as shown in Fig. 40. The same orbit is shown in Fig. 31 (middle right image), where dark material seems to have its origin in a sediment source beneath the crater floors, cut by smaller craters superimposed onto the larger crater's floor. Unfortunately, the DTM does not resolve the exact elevations of the smaller craters supposed to have cut through the subsurface layer, because these smaller craters are beyond the stereo resolution. Nevertheless, the profile provides sufficient insight into the elevation variations of the dark material patches in the craters.

The craters from whose floors dark material emanates are not of the same elevation. The sample profile shows that there is an elevation variation of up to 1337 m between these dark material craters. The red arrows indicate where dark material is visible on the crater floor and might emerge from beneath (elevations from south to north: -4290 m, -4248 m, -4472 m, -4513 m, -4886 m, -5585 m). Moreover, there are regions and craters, which do not show any evidence of dark material at the same or even lower elevations as dark material craters (indicated by green circles). This is particularly conspicuous in the northern part of the observation area. Hence, if there is indeed a dark material source beneath the surface its elevation might vary regionally, so that it either dips to the north below ~5600 m or has been removed completely in this region. An alternative explanation might be an irregular multi-layer source at different elevations. See Chapter VI for a discussion of that hypothesis.

This situation is particularly prevalent in Arabia Terra and Xante Terra. Especially the western and central regions of Arabia Terra provide numerous examples of dark material emerging from crater floors blotched by smaller craters. This region seems to be ideally suited to exhibit and preserve these features, probably due to its elevation and the occurrence of moderately degraded craters. It cannot be ruled out that similar geomorphological signs have been obliterated in more degraded craters, e.g. in the older southern terrains. The northern lowlands generally lack this configuration of crater-blotched impact crater floors.

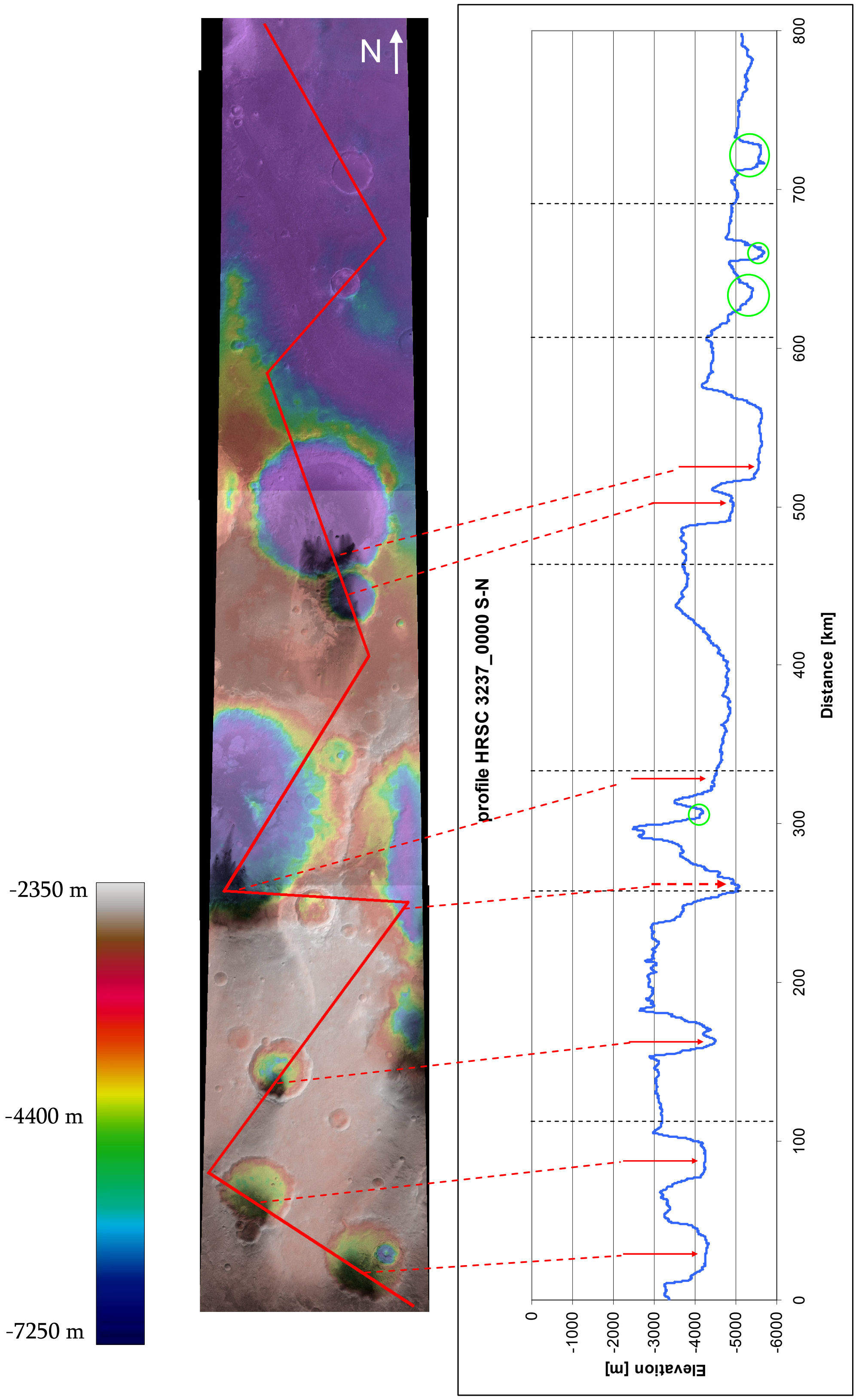

Figure 40: Analysis of the elevations of dark material craters and their surrounding.
Left: Colour-coded HRSC DTM overlaid on HRSC nadir image of orbit 3297_0000 (image width is about 104 km). The red line indicates the course of the profile from south to north. **Right**: corresponding profile along the craters with and without dark material at different elevations. Red dotted lines connect dark material sites in the left-hand image and the right-hand profile (note: the dotted red arrow at about 250 m distance marks the western part of Trouvelot Crater, where dark material is abundant as well [not displayed in this orbit]). The green circles mark regions and craters of lower elevation than the dark material craters which do not show any evidence of dark material. The black dotted lines indicate the breaks in the profile.